Multi-frequential harmonic balance approach for the computation of unsteadiness in multi-stage turbomachines

T. Guédeney[a], A. Gomar[a] and F. Sicot[a]

a. *CERFACS, CFD Team, 42 avenue Gaspard Coriolis 31057 Toulouse cedex 1, France*

Résumé :

Dans les turbomachines, la vitesse relative entre les parties fixes et les parties mobiles génère dans l'écoulement des interactions instationnaires déterministes à une fréquence appelée fréquence de passage des aubes. Dans une turbomachine multi-étagée, une roue aubagée comprise entre deux autres est soumises à (au moins) deux fréquences de passages des aubes, justifiant la nécessité d'une méthode capable de prendre en compte ces instationnarités. Initialement développé pour des problèmes mono-fréquentiels, les méthodes d'équilibrage harmonique ont été étendues afin de prendre en compte des fréquences multiples. Appliquée à une turbomachine multi-étagée, elles permettent de capturer les instationnarités de l'écoulement à un coût 70 fois inférieur par rapport aux méthodes instationnaires classiques.

Abstract :

In turbomachines, the relative motion of fixed and rotating blades gives rise to deterministic unsteady interactions at frequencies termed BPFs (Blade Passing Frequencies). In a multi-stage turbomachine, a row sandwiched between two other rows is submitted to (at least) two BPFs, hence the need for methods able to capture these unsteady effects. Initially developed for single frequency problems, harmonic methods have been extended to account for multiple frequencies. Applied to turbomachines, these methods allows to capture unsteady phenomena of the flow field with a cost four seventy cheaper compared to classical unsteady methods.

Mots clefs : **Harmonic Balance ; Turbomachines ; Row interactions**

1 Introduction

With the need to ever increase performance, aggressive design choices foster unsteady phenomenon, such as : separated flows at or close to stable operability limits, aeroelastic phenomenon, or blade interactions in compact turbo-engines, to name but a few. In such a context, engineers need tools to account for these effects as early as possible in the design cycle. For this reason, efficient and/or accurate unsteady approaches are receiving a lot of attention.

One approach is to improve the time-integration algorithm to reduce the computational cost as compared to standard techniques. To achieve this, Fourier-based methods for periodic flows have undergone major developments in the last decade (see He [10] for a recent review, or the special issue of the International J. of CFD [11]). In this context, the present paper focuses on a time-domain Fourier-based method, namely the Harmonic Balance (HB) method, which transforms an unsteady time-marching problem into the coupled resolution of several steady computations at different time samples of the period of interest.

Initially developed for single (fundamental) frequency problems [9, 6], the HB method has been extended to account for multiple frequencies [7, 2, 3].

The multi-frequential formulation of the HB is first presented, an extension of the chorochronic boundary condition is then described to solve for only one blade passage per row even in a multi-stage turbomachinery. Finally, a multistage compressor case is presented to demonstrate the accuracy and efficiency of the proposed approach for industrial applications.

2 Time-domain almost-periodic harmonic balance technique

The semi-discrete finite-volume form of the Unsteady Reynolds-Averaged Navier-Stokes (U-RANS) equations is given by

$$\frac{d}{dt}\left(VW\right) + R\left(W\right) = 0, \tag{1}$$

where W is the vector of the conservative unknowns (conservative variables and turbulent variables), V the volume of the cell and R the residual resulting from the discretization of the fluxes and the source terms (including the turbulent equations).

If the flow variables are composed of non-harmonically related frequencies (*i.e.* the flow spectrum has high-energy discrete-frequency modes), the flow regime can be termed as almost-periodic [1]. Instead of a regular Fourier series, the U-RANS equations are projected on a set of complex exponentials with arbitrary angular frequencies ω_k. The conservative variables and the residuals are then approximated by

$$W(t) \approx \sum_{k=-N}^{N} \widehat{W}_k e^{i\omega_k t}, \quad R(t) \approx \sum_{k=-N}^{N} \widehat{R}_k e^{i\omega_k t}, \tag{2}$$

where $\widehat{W}_k$ and $\widehat{R}_k$ are the coefficients of the almost-periodic Fourier series for the frequency $f_k = \omega_k/2\pi$. Injecting this decomposition in Eq. (1) yields

$$\sum_{k=-N}^{N} \left(i\omega_k V\widehat{W}_k + \widehat{R}_k\right) e^{i\omega_k t} = 0. \tag{3}$$

Sampling in time onto a set of $2N+1$ time levels to solve Eq. (3), the following matrix formulation is obtained :

$$A^{-1} \cdot \left(iVP\widehat{W}^\star + \widehat{R}^\star\right) = 0, \tag{4}$$

where the almost-periodic inverse discrete Fourier transform (IDFT) matrix reads :

$$A^{-1} = \begin{bmatrix} exp(i\omega_{-N}t_0) & \cdots & exp(i\omega_0 t_0) & \cdots & exp(i\omega_N t_0) \\ \vdots & & \vdots & & \vdots \\ exp(i\omega_{-N}t_k) & \cdots & exp(i\omega_0 t_k) & \cdots & exp(i\omega_N t_k) \\ \vdots & & \vdots & & \vdots \\ exp(i\omega_{-N}t_{2N}) & \cdots & exp(i\omega_0 t_{2N}) & \cdots & exp(i\omega_N t_{2N}) \end{bmatrix}, \tag{5}$$

with $\omega_0 = 0$, $t_0 = 0$, $\omega_{-N} = -\omega_N$ and

$$\begin{aligned} P &= diag\left(-\omega_N, \ldots, \omega_0, \ldots, \omega_N\right), \\ \widehat{W}^\star &= \left[\widehat{W}_{-N}, \ldots, \widehat{W}_0, \ldots, \widehat{W}_N\right]^\top, \\ \widehat{R}^\star &= \left[\widehat{R}_{-N}, \ldots, \widehat{R}_0, \ldots, \widehat{R}_N\right]^\top. \end{aligned} \tag{6}$$

Knowing a time sampling that allows A^{-1} to be invertible, the almost-periodic Fourier coefficients can be approximated thanks to

$$\begin{cases} \widehat{W}^\star = AW^\star, & \text{with } W^\star = \left[W\left(t_0\right), \ldots, W\left(t_i\right), \ldots, W\left(t_{2N}\right)\right]^\top, \\ \widehat{R}^\star = AR^\star, & \text{with } R^\star = \left[R\left(t_0\right), \ldots, R\left(t_i\right), \ldots, R\left(t_{2N}\right)\right]^\top. \end{cases} \tag{7}$$

Equation (4) thus becomes

$$iVA^{-1}PA + R^\star = VD_t[W^\star] + R^\star = 0, \tag{8}$$

where the multiple-frequency HB time-derivative operator $D_t[.] = iA^{-1}PA$, the HB source term, can not be easily derived analytically, and has to be numerically computed.

3 Turbomachinery Application

Under the assumption that all unsteady phenomena in a blade row during stable operation are periodic and can be correlated with the rotation rate Ω of the shaft, the dominant frequencies are those created by the passage of the neighboring blades. In a multi-row turbomachine, a blade row sandwiched between the upstream and downstream rows is subjected to wake and potential effects. In practical turbomachines, the blade counts of neighboring rows are generally different and coprime. Consequently, a sandwiched blade row resolves various combinations of the frequencies, which are additions and/or subtractions of multiples of the blade passing frequencies : according to Tyler and Sofrin [16], the k^{th} frequency in the blade row j is given by

$$\omega_k^{rowj} = \sum_{i=1}^{nRows} n_{k,i} B_i (\Omega_i - \Omega_j). \tag{9}$$

Here, B_i and Ω_i are respectively the blade count and the rotation rate of the i^{th} blade row, $n_{k,i}$ is the k^{th} set of $nRows$ integers driving the frequency combinations. It must be noted that only the blade rows that are mobile relative to the considered j one contribute to its temporal frequencies and that every blade row solves its own set of frequencies and thus its own set of time levels. To set up a HB computation for a multistage configuration, it is of course impossible to use each and every possible $n_{k,i}$, and the user has to choose which frequency combinations will appear in the computation of each row.

3.1 Phase-lagged azimuthal boundary conditions

In a single blade passage computation of a multi-row configuration, the phase-lag condition [4] needs to be used to take the space-time periodicity into account. It states that the flow in one blade passage θ is the same as next blade passage $\theta + \Delta\theta$ but at another time $t + \delta t$:

$$W(\theta + \Delta\theta, t) = W(\theta, t + \delta t), \tag{10}$$

where $\Delta\theta$ is the pitch of the considered row. Assuming that every temporal lag is associated with a rotating wave of rotational speed ω_k, the constant time lag can be expressed as

$$\delta t = \frac{\beta_k}{\omega_k}, \quad \forall k, \tag{11}$$

where

$$\beta_k = 2\pi \text{sign}(\omega_k) \left(1 - \frac{1}{B_j} \sum_{i \neq j} n_{k,i} B_i\right), \tag{12}$$

the $n_{k,i}$ being the integers specified for the computation of the frequencies from Eq. (9), B_i the number of blades in row i and subscript j denoting the current row.

The phase-lag condition was adapted to the time-domain HB by Gopinath *et al.* [6]. The derivation starts with the almost-periodic Fourier transform of Eq. (10) :

$$\sum_{k=-N}^{N} \widehat{W}_k(\theta + \Delta\theta, t)\, e^{i\omega_k t} = \sum_{k=-N}^{N} \widehat{W}_k(\theta, t)\, e^{i\omega_k \delta t} e^{i\omega_k t}. \tag{13}$$

Thus, the flow spectrum from one blade passage is equal to that of the next blade passage modulated by the inter-blade phase angle β_k :

$$\widehat{W}_k(\theta + \Delta\theta, t) = \widehat{W}_k(\theta, t)\, e^{i\omega_k \delta t} = \widehat{W}_k(\theta, t)\, e^{i\beta_k}. \tag{14}$$

Using the same notation as previously, the following matrix formulation is obtained :

$$W^\star = A^{-1} M A W^\star(\theta), \tag{15}$$

where

$$M = diag(-\beta_N, \ldots, \beta_0, \ldots, \beta_N), \tag{16}$$

and A^{-1} is given by Eq. (5).

3.2 Application to a subsonic compressor

In order to validate the non-uniform HB method on a turbomachinery test case, a subsonic compressor case is studied. It is the mid-span slice of the inlet guide vanes (IGV) and the first stage of the axial compressor CREATE [8], located in Lyon (France) at the Laboratoire de Mécanique des Fluides et Acoustique (LMFA). This configuration is composed of 32 IGV blades, 64 rotor (RM1) blades and 96 stator (RD1) blades. The full 3D 3.5-stage computation is presented in Ref. [15].

3.2.1 Mesh and numerical parameters

The blade passages are meshed with a block-structured topology. It is composed of five grid points in the radial direction, 33 in the azimuthal direction and 100 in the axial direction for both rows. This leads to a total number of approximately 50,000 mesh cells.

The IGV blade is not actually meshed but taken into account through a non-uniform injection boundary condition that represents the wake of the IGV entering the RM1 domain. This injection follows the self-similarity law of Lakshminarayana and Davino [12], which states that the spatial evolution of a wake can be described by a Gaussian function. As $B_{RD1} = 3 \cdot B_{IGV}$, the frequency content remains mono-frequential in the rotor (*i.e.*, the BPF of the downstream rotor is just an harmonic of the IGV's BPF). Therefore the number of blades composing the IGV has been changed from 32 to 80 so that the configuration still presents a $2\pi/16$ periodicity but the frequency content is now multi-frequential in the rotor.

The outlet duct is modeled by a valve condition coupled with a simplified radial equilibrium equation. At the blades surfaces, wall laws [5] are imposed. The lower and upper radial conditions are slip walls.

The convective fluxes are discretized using the second-order Jameson scheme with added artificial viscosity, or a second-order Roe scheme. For this study, the turbulent viscosity is computed with the one-equation model proposed by Spalart and Allmaras.

The DTS scheme is used to get a numerical reference solution. The periodicity of the different blade passages is such that a $2\pi/16$ periodicity is enough to perform the unsteady computations. To reach an established periodic state, 67 passages (using 400 instants per azimuthal period) of the periodic sector are necessary.

3.2.2 Results

Two sets of frequencies (one of four and one of six frequencies), are chosen to run the harmonic balance computations. They are summarized Tab. 1.

Figure 1 shows the instantaneous entropy flow field for the maximum-efficiency operating point $\eta^*_{is} = 1$. For the HB computations, the computed passage is duplicated using phase-lag to check that the azimuthal phase-lag boundary conditions ensure the continuity of the flow field between the original blade passage and the duplicated ones. All the wakes are correctly convected downstream and very few differences can be seen in the different flow fields. Some numerical wiggles can be observed downstream the RM1/RD1 interface, but the higher the number of frequencies, the better the solution, as already shown by Sicot *et al.* [14].

	n IGV	n RM1	n RD1	Initialization
$N = 4$	1	1	0	Restart from steady computation
	0	2	1	15,000 it. in Roe second order scheme
	2	3	0	then 10,000 it. in Jameson scheme
	0	4	2	
$N = 6$	1	1	0	
	0	2	1	Restart from $N = 4$
	2	3	0	5,000 it. in Jameson scheme k_4=0.064
	0	4	2	then 5,000 it. in Jameson scheme k_4=0.032
	3	5	0	
	0	6	3	

TABLE 1 – Frequency combination coefficients to compute only harmonics of the fundamental blade-passing frequencies.

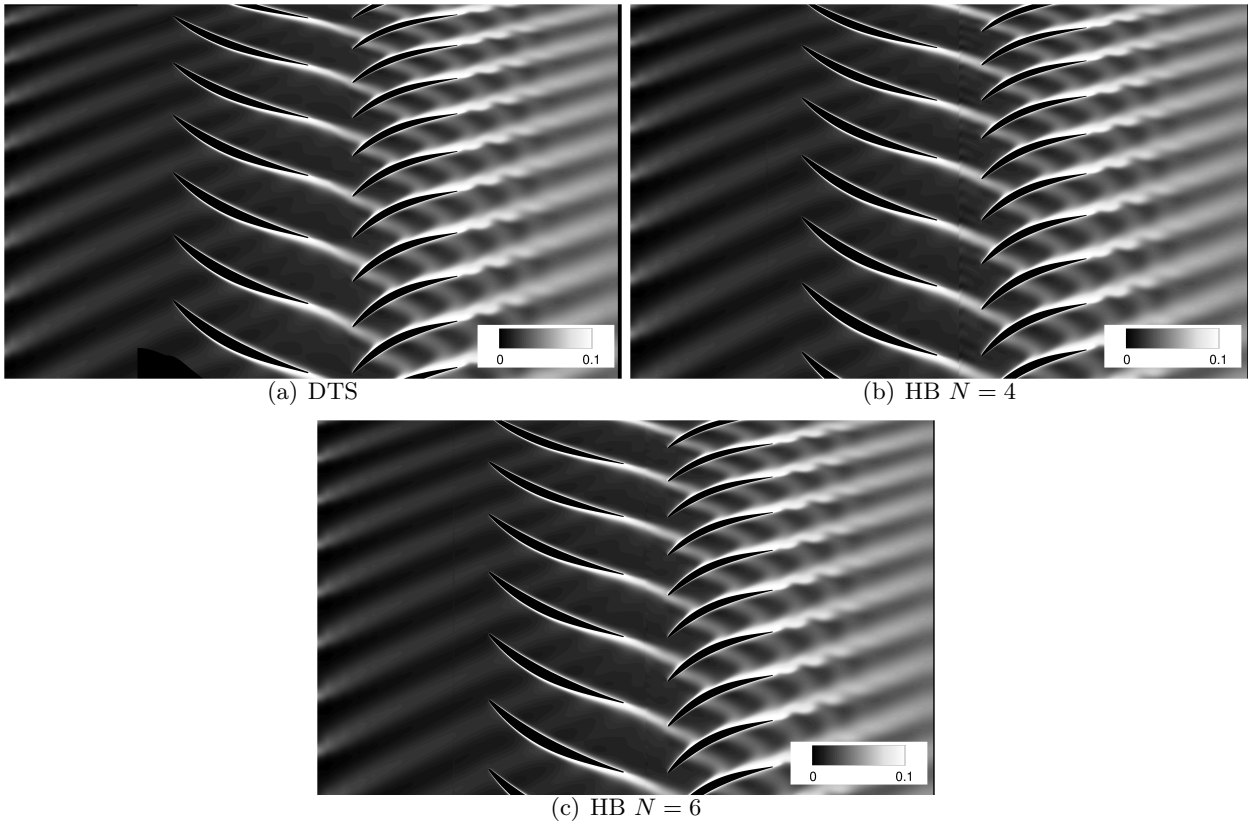

(a) DTS (b) HB $N = 4$

(c) HB $N = 6$

FIGURE 1 – Comparison of the entropy flow field at $\eta_{is}^* = 1.0$ and $t = 0$.

3.2.3 Computational gain

The HB computations allow a reduction of the CPU cost by a factor 4.5 for four frequencies and 2 for the six frequencies set, the gain being higher with fewer harmonics. However, it should be kept in mind that the reference DTS simulations are done on a $2\pi/16$ periodic sector, whereas practical turbomachinery configurations usually do not have such periodicity, thus requiring simulations on the whole 360° machine. In this case, an additional factor 16 in gain can thus be estimated, suggesting a gain of almost two orders of magnitude.

4 Conclusions

A multi-frequential harmonic balance approach is presented. The flow in a multi-stage axial compressor is computed to prove the maturity of the method. It is shown that nonlinear flows can be modeled to engineering accuracy with only four frequencies. In the present case, the HB method is about 70 (4.5×16) times faster than a classical time-marching computation over the whole annulus, thanks to the efficient spectral-integration scheme and to the generalized phase-lag boundary conditions. The conclusions obtained for the present quasi-2D case have been extended to 3D geometries without any new assumption [13].

Références

[1] A. S. Besicovitch. *Almost Periodic Functions*. Cambridge University Press, 1932.

[2] K. Ekici and K. C. Hall. Nonlinear Analysis of Unsteady Flows in Multistage Turbomachines Using Harmonic Balance. *AIAA Journal*, 45(5) :1047–1057, 2007.

[3] K. Ekici and K. C. Hall. Nonlinear Frequency-Domain Analysis of Unsteady Flows in Turbomachinery with Multiple Excitation Frequencies. *AIAA Journal*, 46(8) :1912–1920, 2008.

[4] J. I. Erdos, E. Alznert, and W. McNally. Numerical Solution of Periodic Transonic Flow through a Fan Stage. *AIAA Journal*, 15(11) :1559–1568, November 1977.

[5] E. Goncalves and R. Houdeville. Reassessment of the Wall Function Approach for RANS Computations. *Aerospace Science and Technology*, 5 :1–14, 2005.

[6] A. Gopinath and A. Jameson. Time Spectral Method for Periodic Unsteady Computations over Two- and Three- Dimensional Bodies. In *43rd Aerospace Sciences Meeting and Exhibit*, Reno (USA), January 2005. AIAA Paper 2005-1220.

[7] A. Gopinath, E. Van Der Weide, J.J. Alonso, A. Jameson, K. Ekici, and K.C. Hall. Three-Dimensional Unsteady Multi-Stage Turbomachinery Simulations using the Harmonic Balance Technique. In *45th AIAA Fluid Dynamics Conference and Exhibit*, Reno (USA), 2007. AIAA Paper 2007-0892.

[8] N. Gourdain, X. Ottavy, and A. Vouillarmet. Experimental and Numerical Investigation of Unsteady Flows in a High Speed Three Stage Compressor. In *8th European Turbomachinery Conference*, Graz (Austria), March 2009. B 107.

[9] K. C. Hall, J. P. Thomas, and W. S Clark. Computation of Unsteady Nonlinear Flows in Cascades using a Harmonic Balance Technique. *AIAA Journal*, 40(5) :879–886, 2002.

[10] L. He. Fourier Methods for Turbomachinery Applications. *Progress in Aerospace Sciences*, 46(8) :329–341, 2010.

[11] Li He, editor. *Special Issue : Fourier-Based Method Development and Application*, volume to appear. International Journal of Computational Fluid Dynamics, 2013.

[12] B. Lakshminarayana and R. Davino. Mean Velocity and Decay Characteristics of the Guide Vane and Stator Blade Wake of an Axial Flow Compressor. In *Gaz Turbine Conference and Exhibit and Solar Energy Conference*, San Diego (USA), 1979. ASME Paper 79-GT-9.

[13] F Sicot, T. Guedeney, and G. Dufour. Time-Domain Harmonic Balance Method for Aerodynamics and Aeroelastic Simulations of Turbomachinery Flows. *International Journal of Computational Fluid Dynamics*, In press, 2013.

[14] Frederic Sicot, Guillaume Dufour, and Nicolas Gourdain. A Time-Domain Harmonic Balance Method for Rotor/Stator Interactions. *Journal of Turbomachinery*, 134(1) :011001, 2012.

[15] Frederic Sicot, Thomas Guedeney, and Guillaume Dufour. Time-domain harmonic balance method for aerodynamics and aeroelastic simulations of turbomachinery flows. *International Journal of Computational Fluid Dynamics*, 2012.

[16] J.M. Tyler and T.G Sofrin. Axial Flow Compressor Noise Studies. *Society of Automotive Engineers Transactions*, 70 :309–332, 1962.